Decreased Sensitivity of Grassland Spring Phenology to Temperature on the Tibetan Plateau

Zhangkai Chen, Rui Chen, Yajie Yang, Huiqin Pan, Qiaoyun Xie, Cong Wang, Baodong Xu, and Gaofei Yin, *Senior Member, IEEE*

***Abstract*—Spring phenology is a critical indicator to characterize vegetation dynamics and their responses to climate change. Spring phenology on the Tibetan Plateau (TP) has received extensive attentions as it has experienced one of the most rapid warmings. Warming-induced advancement of spring phenology has been revealed by many studies, however, the underlying mechanisms remain obscure. In this article, we derived the start of growing season (SOS) from the satellite solar-induced chlorophyll fluorescence (SIF) and investigated the spatial and temporal variations of SOS over grasslands on the TP during 2001–2020. The temperature sensitivity (St) of SOS was then analyzed, i.e., the slope of a linear regression between the advanced SOS and preseason air temperature. Results showed an average advanced trend of 0.29 days per decade of SOS, although not statistically significant. Spatially, grasslands in eastern TP showed an earlier trend of SOS whilst those in western TP showed a later trend of SOS. The spatial distribution of St was much more affected by precipitation and air temperature, i.e., a 1 mm decrease of precipitation and 1 °C warming incur a decrease in St of 0.02 and 0.54 day/°C, respectively. Temporally, St showed a significant decrease with an average speed of 0.14 day/°C per year during 2001–2020, and the climate controllers show a high spatial heterogeneity. These findings improved our understanding of grasslands spring phenology responses to warming and help us clarify future global water and energy cycles.**

***Index Terms*—Solar-induced chlorophyll fluorescence (SIF), spring phenology, temperature sensitivity (St), Tibetan Plateau (TP).**

Manuscript received 21 February 2023; revised 7 April 2023; accepted 19 April 2023. Date of publication 25 April 2023; date of current version 15 May 2023. This work was supported in part by the National Key Research and Development Program of China under Grant 2019YFE0126700, in part by the National Natural Science Foundation of China under Grant 42271323 and Grant 41971282, and in part by the Sichuan Science and Technology Program under Grant 2021JDJQ0007 and Grant 2020JDTD0003. *(Corresponding author: Gaofei Yin.)*

Zhangkai Chen, Rui Chen, Yajie Yang, Huiqin Pan, and Gaofei Yin are with the Faculty of Geosciences and Environmental Engineering, Southwest Jiaotong University, Chengdu 610031, China (e-mail: zhangkaichan@163.com; chenrui960301@my.swjtu.edu.cn; yajiey@my.swjtu.edu.cn; hqp9600@163.com; yingf@swjtu.edu.cn).

Qiaoyun Xie is with the School of Engineering, The University of Western Australia, Perth, WA 6005, Australia (e-mail: Qiaoyun.Xie@uwa.edu.au).

Cong Wang is with the Key Laboratory for Geographical Process Analysis & Simulation of Hubei Province/School of Urban and Environmental Sciences, Central China Normal University, Wuhan 430079, China (e-mail: wangcong@ccnu.edu.cn).

Baodong Xu is with the Macro Agriculture Research Institute, College of Resources and Environment, Huazhong Agricultural University, Wuhan 430070, China (e-mail: xubaodong@mail.hzau.edu.cn).

This article has supplementary downloadable material available at https://doi.org/10.1109/JSTARS.2023.3269908, provided by the authors.

Digital Object Identifier 10.1109/JSTARS.2023.3269908

I. Introduction

SPRING phenology is a highly sensitive indicator to characterize vegetation dynamics and their responses to climate change [1], [2], [3]. Climate change has an impact on spring phenology, and phenological changes regulate vegetation's ability to feed back to the climate system through affecting the carbon, water and energy cycles [4], [5]. Therefore, it is crucial to comprehend the probable mechanisms of climate factors influencing spring phenology in order to improve phenology prediction in future climate change, which may help us in better understanding future carbon, water and energy cycles.

The Tibetan plateau (TP), the highest plateau in the world, has warmed at one of the fastest rates (~ 0.4 °C per decade), which is twice the average rate of global warming [2], [6]. Several studies have indicated early spring phenology in response to spring warming in the grasslands of TP since the 1980s [7], [8], [9], which was also found in other high-elevation and high-latitude regions [10], [11], [12]. However, due to the ambiguity created by many data sources and the shifting relative importance of climate limitations on spring phenology, it is elusive whether this accelerated spring phenology trend will continue into the 21st century [13]. For instance, recent studies have reported that spring phenology was overestimated by the structural vegetation indices [e.g., normalized difference vegetation index (NDVI) and enhanced vegetation index (EVI)] [14], [15], and these indices were impacted by cloud, snow, or ice cover [14]. The new solar-induced chlorophyll fluorescence (SIF), in contrast to conventional vegetation indices, provides a direct measure of photosynthesis as it is released from the chlorophyll of photosynthesis-sensitive plants [13]. As a result, SIF is less likely to be impacted by cloud, snow and other environmental factors [13], [14]. In addition, previous studies have also reported the strong linear correlation between SIF and GPP for various biomes including crops, grasslands, and temperate forests on the TP [16], [17], [18], providing a potential way for detecting vegetation phenology at large scales from photosynthetic perspective [16], [19].

The temperature sensitivity (St), defined as the advancement of spring phenology in response to a unit shift in preseason air temperature [1], has been widely used for assessing and predicting phenology responses to climate change [8], [10], [20], [21]. Previous researches using *in situ* observations revealed that St generally decreased with increasing spring temperatures [1], [22], [23], [24]. However, our knowledge of how increasing

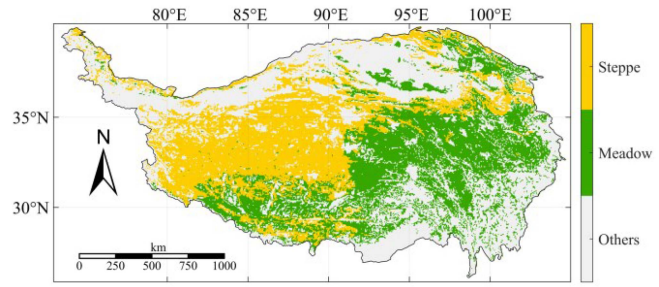

Fig. 1. Spatial distribution of grasslands on the Tibetan Plateau.

temperature regulates spring phenology as well as St variations for grasslands on the TP since 2000s is still poor, especially regarding the underlying mechanisms behind spring phenology responses to climate change on the TP [5], [8], [25], [26], [27].

In this article, we took advantage of SIF to extract grassland spring phenology [i.e., start of growing season (SOS)] on the TP and revealed the spatial and temporal variations of St from 2001 to 2020. To investigate the underlying determinants of the TP grasslands' responses to climate change and facilitate our understanding of these ecosystems in future climates, we aimed to: investigate spatial and temporal patterns of SOS trends derived from SIF time series from 2001 to 2020; elucidate the response of SOS to preseason air temperature (i.e., St) and the effects of preseason climate factors in determining the spatial pattern of St; and investigate the temporal variation of St and underlying climate controllers.

II. Materials and Methods

A. Study Area

The TP is located in western China (25. 9°N $\sim$ 40.0°N, 73. 4°E $\sim$ 104. 3°E), accounting for approximately 15% of the land area in China [28]. As the highest land of the world, TP has an average altitude of over 4000 m, a typical cold climate, little precipitation, significant solar radiation and thin air (see Fig. 8) [5], [29], [30]. The dominant land covers are steppe and meadow, which respectively covers 28.2% and 28.6% of the entire TP, according to the Vegetation Maps of China with a scale of 1:1000000 (see Fig. 1) [31], [32]. In this article, we focused on the grasslands area (i.e., steppe and meadow).

B. Datasets

1) Contiguous Solar-Induced Fluorescence Data: The contiguous solar-induced fluorescence data (CSIF) was selected to extract SOS, which was freely acquired from National Tibetan Plateau Third Pole Environment Data Center (TPDC, http://data.tpdc.ac.cn/en/data/d7cccf31-9bb5-4356-88a7-38c5458f052b/). CSIF is produced by a machine learning method from orbiting carbon observatory-2 SIF dataset and MODIS (Moderate-resolution Imaging Spectroradiometer) reflectance dataset (MCD43C1 C6), with the spatial resolution of 0.05° and the temporal resolution of 4-days, available from 2001 to 2020 [33]. In this article, we selected the clear-sky daily CSIF ($\text{CSIF}_{\text{clear-daily}}$) since it has a good performance validated by original SIF observations (Coefficient of determination, $R^2 = 0.79$), and also has high correlations with GPP estimated from flux towers [33]. To match the resolution of the climate dataset, we resampled the CSIF data to 0.1° by a 2×2 window averaging method.

2) ERA-5 Land Climate Reanalysis Dataset: In this article, the hourly 2 m air temperature, precipitation and shortwave downward radiation data from 2001 to 2020 with a spatial resolution of 0.1°×0.1° were employed from ERA5-Land climate reanalysis dataset, which was developed by the European Centre for Medium-Range Weather Forecasts (ECMWF) Website (https://cds.climate.copernicus.eu/cdsapp#!/dataset/reanalysis-era5-land) [34]. The ECMWF ERA5 climate reanalysis' land component was replayed to create ERA5-Land dataset, which offered a more consistent depiction of the evolution of land variables across multiple decades than ERA5 [34], [35]. We synthesized the hourly ERA5-Land data into daily data.

3) Landcover Dataset: The Vegetation Maps of China with a scale of 1:1000000 was used to identify land cover types in our study area. Alpine meadows and alpine grasslands are included in this data as grasslands, which are more suited for TP research than other land cover products [5], [7]. This dataset was provided by Environmental & Ecological Science Data Center for West China, and can be freely available from http://westdc.westgis.ac.cn. We merged the alpine meadow and steppe into a simplified "grasslands" class.

C. Methods

1) Extraction of the Start of Growing Season: To avoid systematical error of different phenological extraction methods, we used two widely used methods, i.e., dynamic threshold and double logistic function method to extract SOS [5].

a) Dynamic threshold method: To lessen the bias caused by random noise, we first linearly interpolated the 4-days of CSIF data to create a daily time-series, and then we smoothed it using Savitzky–Golay (S–G) and harmonic analysis of time series (HANTs) filtering [36], [37]. To guarantee the smoothness of the CSIF time series, a 32-day window was chosen in S–G filtering [15]. The parameters of the HANTs filter were referenced from Zhou et al. [38]. In this article, 20% of CSIF value was used to extract SOS on the TP [2], [39], [40], [41]

$$\text{CSIF}_{\text{ratio}} = \frac{(\text{CSIF}_{ts} - \text{CSIF}_{\min})}{(\text{CSIF}_{\max} - \text{CSIF}_{\min})} \tag{1}$$

where CSIF_{ts} is the value of CSIF in the smoothed time series *ts*; and the $\text{CSIF}_{\max}$ and $\text{CSIF}_{\min}$ are the maximum and minimum value of the CSIF in the smoothed time series of current annual year, respectively. The SOS was specifically defined as the average first day of the *ts* when $\text{CSIF}_{\text{ratio}}$ value exceeds 0.2.

b) Logistic function method: The logistic function method is predicated on the idea that vegetation growth follows a well-defined temporal profile. As a result, the time series CSIF (smoothed by S–G) can be fitted by a logical function, such as

double logistic function as follows [10], [42], [43], [44]:

$$f(ts) = \mathrm{CSIF}_w + \frac{\alpha_S}{1 + e^{-\partial S \times (ts - S)}} - \frac{\alpha_A}{1 + e^{-\partial A \times (ts - A)}}. \quad (2)$$

In the (2), *f(ts)* is the fitted CSIF at the date (day of year, DOY) *ts*, CSIF_w is the base winter CSIF, α_S and α_A represent the amplitudes of spring green-up and autumn brown-down plateau, respectively. The transition curvature parameters are δ_S (which corresponds to the spring plateau) and δ_A (which corresponds to the autumn plateau), and *S* and *A* are the transitions' DOY midpoints for green-up and brown-down, respectively [43]. Moreover, by using least squares method, the parameters (α_S, α_A, δ_S, δ_A, *S*, *A*) were fitted against actual observations [45]. In this method, SOS is estimated by using the minimum and maximum values of the first, second, and third derivatives [43], [45], i.e.,

$$\mathrm{SOS} = S - 4.562/2 \times \mathrm{CSIF}_w \quad (3)$$

where *S* and CSIF_w are fitted parameters in (2). Finally, we averaged the SOS obtained by above-mentioned two methods as the final SOS.

2) Calculation of the Temperature Sensitivity (St): Temperature sensitivity (St) is the main effective and simple way to evaluate phenology responses to climate warming [1], [12], [24]. In this article, the slope of a linear regression of advanced spring phenological days versus preseason temperature was used to determine the St of spring phenology [1], [10], [24], [46]. As a result, "preseason" refers to the climatic conditions that the vegetation was exposed to the date before the SOS [23]. The "preseason length" was defined as the date from November 1st in preceding year to the SOS of current year, and air temperature corresponding to the preseason length is the preseason temperature [1], [47]. Likewise, we defined preseason precipitation and radiation in the same way. In this article, a positive value of St indicates warming-induced advancement of SOS (i.e., earlier SOS), and vice versa.

3) Statistical Analysis: To examine the monotonic trends in SOS and St and determine their significance, we employed the Theil–Sen method and the Mann–Kendall (MK) trend test [48], [49]. Details regarding the above-mentioned two methods could be found in Jiang et al. [48]. When analyzing trends of SOS, we also highlighted trends that the MK trend test indicated were significant at the 5% confidence level ($p < 0.05$).

In addition, simple linear regressions [22] were used to calculate correlations between the spatial distribution of St and preseason climate factors. And we analyzed temporal changes of St by using decadal differences and a 5-year moving window, respectively. We calculated the change of St by comparing the sign of the two generational St value, which determines the decadal difference of St (same sign means no significant change, and the different sign means significant change).The t-test [50] and MK trend test were used for significance test of St. Moreover, the contributions of climate factors (preseason temperature, precipitation and radiation) to St were evaluated by using partial regression models. We ordered these factors (i.e., climatic factors) according to the absolute value of their partial correlation coefficients to identify the factors that contributes the most to the St dynamics. The main contributor to the St in that grid cell was determined to be the factors with the biggest absolute value of partial correlation.

III. Results

A. Spatio-Temporal Dynamics of Spring Phenology on the Tibetan Plateau

In general, the multi-averaged SOS during 2001–2020 ranged from April to June from the eastern to the western TP [see Fig. 2(a)]. The trend of SOS revealed distinct spatial patterns between eastern and western TP [see Fig. 2(b)]. About 58.1% of the grasslands area exhibited advanced/earlier trends in SOS, which mainly located in the eastern TP, among which 9.2% was significant. On the contrary, the delayed SOS (41. 9%) was distributed at the southwestern TP, and the significant trend accounted for 2.6%. Overall, SOS had an average advancement of 0.29 days *per* decade for grassland ecosystems on the entire TP.

B. Spatial Pattern of Temperature Sensitivity of Grassland Spring Phenology

The temperature sensitivity (St) during 2001–2020 was presented in Fig. 3. Overall, the average St over grasslands on the TP is approximately 0.66 day/°C, which means an increase in preseason temperature of 1 °C corresponded to an advancement of 0.66 days in SOS. The St showed an apparent distinct spatial pattern over grasslands on the TP, which was similar with the spatial pattern of SOS trend [see Fig. 2(b)]. In the southwest of TP, the majority of pixels exhibited negative St, with the mean value of −5.47 day/°C. In contrast, positive St was mainly concentrated in the center and east of TP, accounting for about 58% of the grasslands of TP, most of which were higher than +3 day/°C.

We further investigated the distribution of St with a combination of preseason climate factors (i.e., preseason temperature, precipitation and radiation). About 80.3% of TP grasslands showed an increasing trend of preseason temperature at an average rate of 0.03 °C per year, which was larger in the western than that in the eastern TP [see Fig. 9(a) and (b)]. Likewise, preseason radiation showed an apparent increase trend with about 72.3% regions of grasslands on the TP [see Fig. 9(e) and (f)]. On the contrary, preseason precipitation showed a significant decrease for 59.1% of grasslands on the TP [see Fig. 9(c) and (d)].

We observed that St has obvious distribution differences in a climatic space composed of temperature and precipitation (see Fig. 4). The negative St was mainly occurred in the regions with preseason precipitation lower than 200 mm and preseason temperature higher than 0 °C (see Fig. 4). Positive St was mainly occurred in cold (preseason temperature < 0 °C) and humid/sub-humid (preseason precipitation > 200 mm) regions (see Fig. 4). Preseason precipitation was highly and positively correlated with St ($R^2 = 0.81$), while the negative correlations ($R^2 = 0.78$) were found for preseason temperature. Moreover, similar relationships were also observed in radiation and

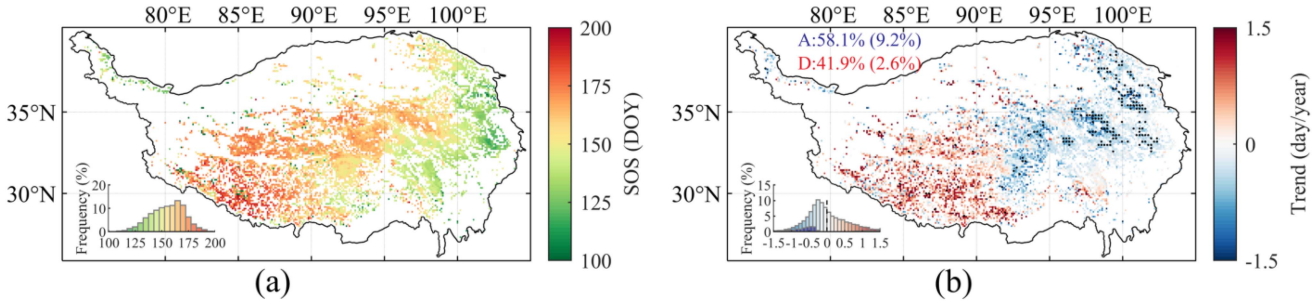

Fig. 2. Spatial pattern of (a) the multiaveraged SOS and (b) temporal trends of SOS during 2001–2020. The bottom left insets show the corresponding frequency distributions. The texts in (b) show the proportions of areas with advanced (A) and delayed (D) SOS, with the significant pixels ($p < 0.05$) indicated in the bracket.

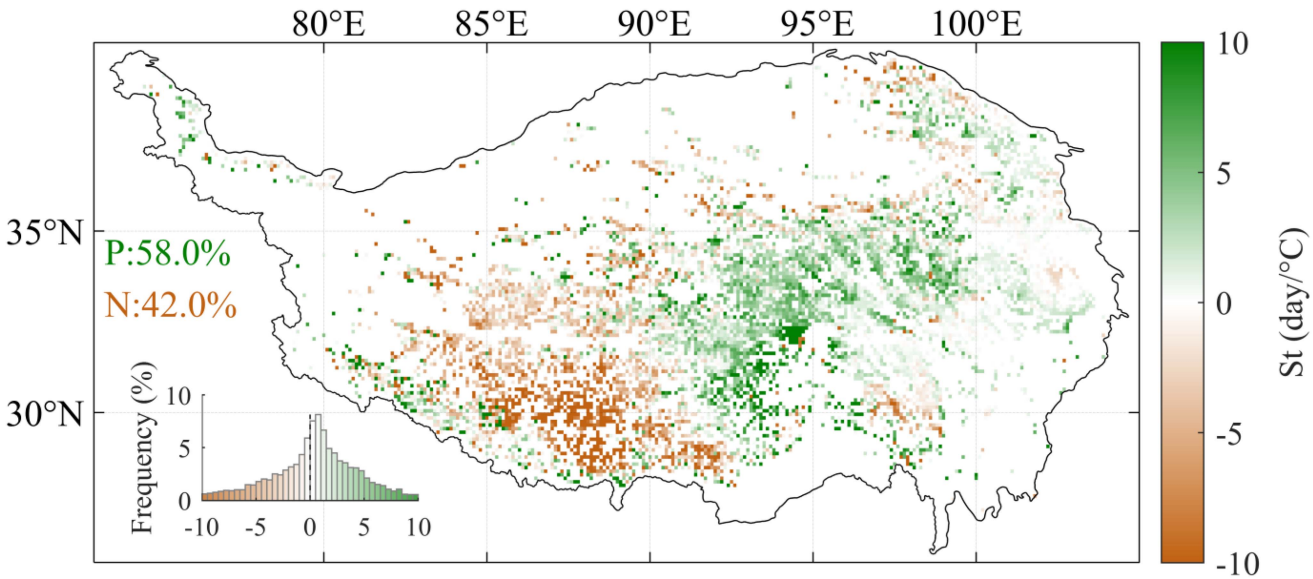

Fig. 3. Spatial pattern of temperature sensitivity (St) on the Tibetan Plateau during 2001–2020. The bottom left insets show the frequency distributions of St, and the texts show the proportions of areas with positive (P) and negative (N) St, respectively.

precipitation (see Fig. 10), but not in temperature and radiation (see Fig. 11). Overall, the spatial distribution of St was much more affected by the ambient conditions of temperature and precipitation than radiation, with a 1 mm decrease of precipitation and 1 °C warming incur a decrease in St of 0.02 and 0.54 day/°C, respectively.

C. Decreased Temperature Sensitivity of Grassland Spring Phenology

We found that the percentage of positive St decreased from 64.8% in 2001–2010 to 50.4% in 2011–2020 [see Fig. 5(a) and (b)]. That is, about 44.7% of grasslands spring phenology on the TP have experienced distinct shift in St. At the same time, the mean value of St in 2001–2010 was much higher than that in 2011–2020 (+1.38 day/°C *vs.* +0.16 day/°C), and the difference of St in the two decades are significant at a level of $p < 0.01$ [see Fig. 5(c)]. Trend analysis by a 5-year moving window from 2001 to 2020 presented that St decreased by an average speed of 0.14 day/°C *per* year ($p = 0.1$) [see Figs. 6 and 12]. These results highlighted that the St of grasslands spring phenology on the TP have experienced obviously decrease in the past two decades.

D. Attribution of Temporal Decrease in Temperature Sensitivity

We further explored the contributions of preseason climate factors to the decrease of St by partial correlation analysis based on the St calculated by 5-year moving window. Considering the length of the moving window may affect the trend of St, we tested six different sizes of moving windows. The results showed that a 5-year moving window was the most suitable method to calculate the temporal change of St (see Fig. 13). Partial correlation analysis allowed us to control the influence of other factors when analyzing the correlation between climate factor and St. Preseason temperature showed negative partial correlation with St for 56.5% grasslands on the TP (10.7% was significant at

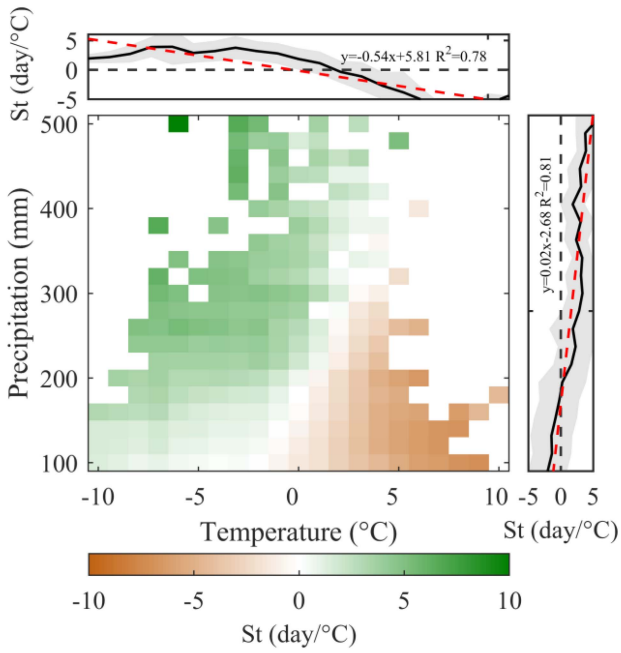

Fig. 4. Distribution of temperature sensitivity (St) in the climatic space composed of the preseason temperature and preseason precipitation during 2001–2020. In the upper and right subgraphs, the solid black lines indicate the St variations with temperature and precipitation, respectively. The gray shadows areas the standard deviation error of St in each bin, the dashed red lines are the fitted linear regressions, and the dashed black lines indicate the location of 0 day/°C.

$p < 0.05$ level), which mainly distributed in southwest and center of TP [see Fig. 7(a)]. This relationship might indicate that increasing preseason temperature will shift St to negative direction, that is, warming would be less beneficial to vegetation growth in these areas. Likewise, Preseason precipitation showed negative partial correlation with St in about 56.6% regions (7.5% was significant at $p < 0.05$ level) [see Fig. 7(b)]. Preseason radiation showed positive relationship with St in about 52.0% regions (7.6% was significant at $p < 0.05$ level) [see Fig. 7(c)]. The results of corresponding areas of each dominant/limiting factor are presented in Fig. 7(d). For the entire TP, the St was limited by preseason temperature, radiation and precipitation in 37.9%, 34.4%, and 27.7% of the areas, respectively.

IV. Discussion

A. Spatio-Temporal Variation of Grassland Spring Phenology

This article estimated the SOS and its temporal variation over the grasslands on the TP from 2001 to 2020 based on CSIF data. We found that SOS in the western TP was generally later than that in the eastern part. In the western TP, the sparse vegetation and relatively high temperature induced larger evapotranspiration and lower accumulated preseason precipitation [28], [39]. Vegetation growth was inhibited and vegetation takes longer to end the dormant period, resulting in delayed spring phenology on the western TP [2]. On the contrary, relatively sufficient precipitation could meet the water demand for vegetation growth, and low-risk drought allowed vegetation to benefit more in terms of temperature on the eastern TP [51]. Besides, we found that the spatial pattern of SOS was roughly consistent with that of the two grassland types, which might indicate that the spring phenological changes of grasslands were contributed by grassland types on the TP [52].

Our results confirmed the spatial distribution of different trends of SOS in the eastern and western TP during the period 2001–2020, which was apparently consistent with previous studies [2], [5], [13], [53]. Recent studies gave possible explanations about the opposite trends on the TP: The ecosystems in the east and west were under stress from the cold and the drought, respectively [2], [13]. In the eastern TP, the daily average temperature was consistently below 0 °C from November until the following April on the TP [2]. Thus, an increasing spring temperature would advance the green-up date (corresponding to SOS) of alpine vegetation. In the western TP, increasing forcing temperature did not necessarily advance SOS due to the impact of decrease in preseason precipitation [53]. Our results identified that SOS showed no significant trends with an average advancement of 0.29 days *per* decade on the TP. This finding may put an end to the discussions about whether spring phenology has continuously advanced in climate-sensitive regions (e.g., TP) into the 21st century [53], [54].

B. Spatial Variation of Temperature Sensitivity

We observed that the spatial distribution of St was much more affected by the ambient conditions of temperature and precipitation, which was highly correlated with preseason precipitation ($R^2 = 0.81$) and temperature ($R^2 = 0.78$) on the TP. In arid/semi-arid regions (preseason precipitation < 200 mm), soil moisture might remain suboptimal after low rainfall, and continued warming could lead to even harsher vegetation growth conditions. Thus, St was more correlated with preseason precipitation than preseason temperature in these regions [51]. Furthermore, preseason high temperatures in arid/semiarid regions might lead to increased evapotranspiration and thus less water availability, which might result in the delay of SOS [55], explaining the negative St observed in grasslands in arid/semi-arid regions on the western TP. By contrast, in humid/sub-humid regions (preseason precipitation > 200 mm), the initiation of vegetation growth was not limited by water shortage, and as a result, the St was more correlated with preseason temperature than to preseason precipitation. In these regions, St was positive under increasing preseason temperature.

C. Temporal Decrease of Temperature Sensitivity

Previous studies have reported that St has experienced a significantly decrease on hemisphere and regional scales in the past decades [1], [22], [24]. Our results suggested that St of grassland significantly decreased with the speed of 0.14 day/°C per year on the TP from 2001 to 2020, which was faster than Central European (0.07 day/°C per year) and Switzerland (0.05 day/°C per year) [1], [24].

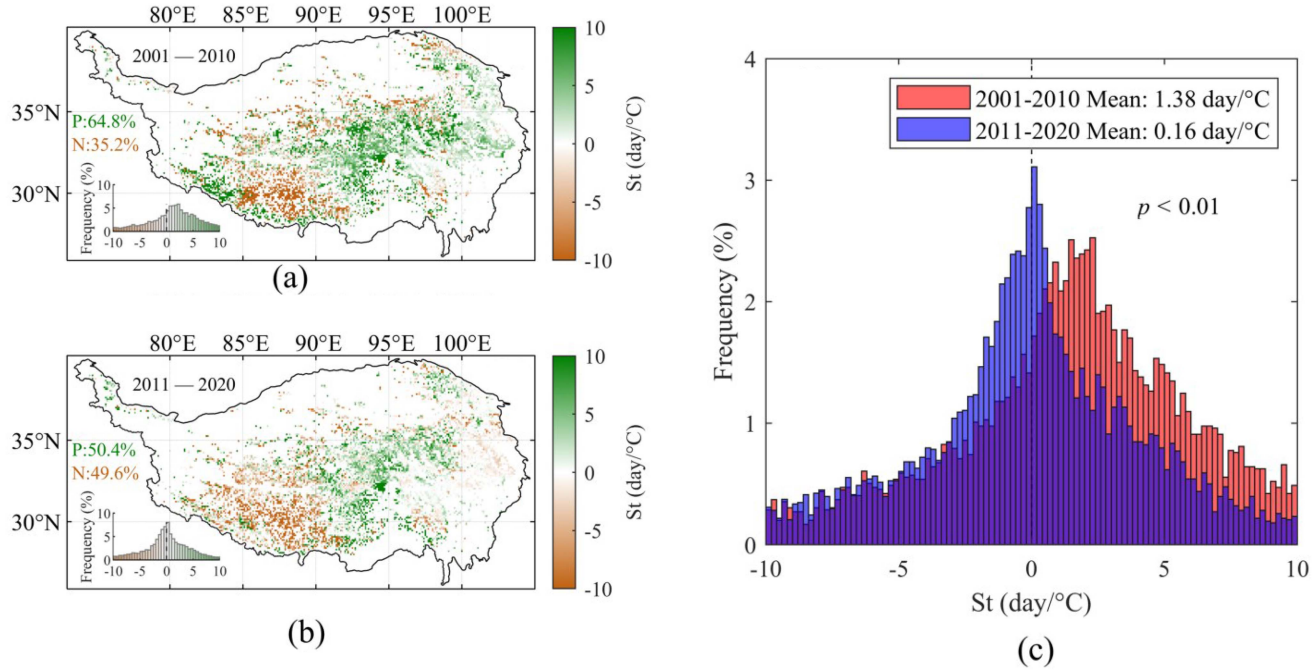

Fig. 5. Spatial pattern of temperature sensitivity (St) for periods of (a) 2001–2010 and (b) 2011–2020, (c) St distributions of the two decades. The texts in (c) show the p value of t-test of decadal St and decadal-averaged St.

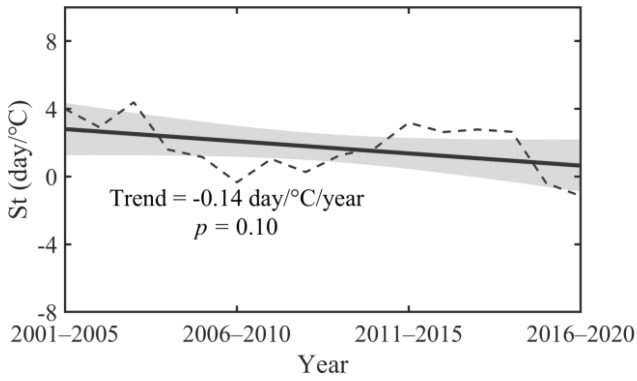

Fig. 6. Temporal variation of temperature sensitivity (St) with a 5-year moving window on the Tibetan Plateau during 2001–2020. The trend (fitted by simple linear regression) and the significance level were indicated in the figure.

The St was co-controlled by preseason temperature (37.9%), radiation (34.4%) and precipitation (27.7%) during 2001–2020 [see Fig. 7(d)]. Previous studies showed that preseason temperature and radiation would be an important climate factor that would dominate the temporal decrease of St [22], [24], which was consistent with our finding. However, the dominant climatic factor controlling St was spatially heterogeneous. We provided possible potential mechanisms for interpreting the decrease in St on the TP.

First, vegetation needs heat accumulation after emerging from dormancy to start leaf unfolding in spring [1]. At the same time, vegetation needs to break dormancy in order to spread leaves, which requires sufficient chilling accumulation during dormancy [4], [53]. In the context of continuous global warming, the chilling accumulated during the dormancy period reduced, thus increasing the heat demand and slowing down the leaf unfolding [1], [56]. The lack of chilling prolonged the dormant period of vegetation and led to the slowing down of spring phenological advance (i.e., slowing downing the advancement of SOS).

Second, the indirect influence on SOS can be used to explain how radiation and precipitation regulate St [22], [57]. In several studies, it has been demonstrated that radiation indirectly influences spring phenology because it affects temperature and moisture by regulating heat flux and evapotranspiration [22], [58]. Increasing preseason radiation strength the solar-induced warming, resulting in additional increases in turbulent fluxes and evapotranspiration [59], and the decrease of preseason precipitation leads to the decrease of vegetation available water [1], [60], [61]. These effects limited vegetation growth in spring and slow down the advanced trend of SOS, which reducing the sensitivity of vegetation response to warming.

In addition, photoperiod limitation mechanisms and vegetation adaptation may also limit when leaf unfolding dates occur too early in the season, which influences temporal variation in St [22], [24].

D. Limitations and Future Work

Our study revealed different potential mechanisms of grassland spring phenology and St variations on the TP. It was notable that many of the explanations in our study were speculative and

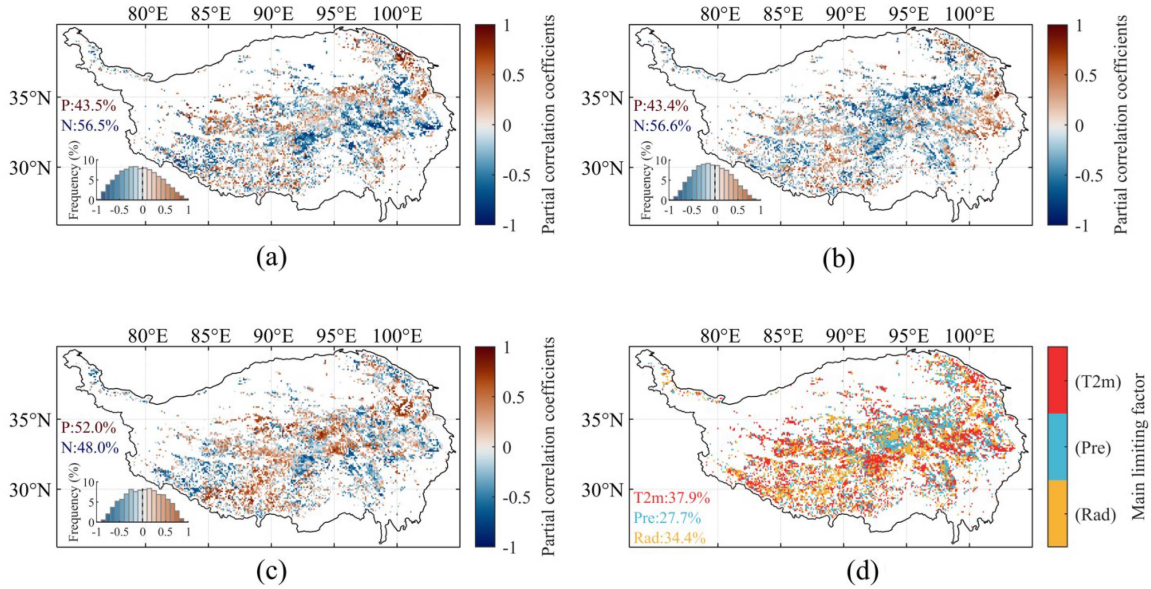

Fig. 7. Spatial pattern of partial correlation coefficient between the temperature sensitivity (St) and preseason (a) temperature, (b) precipitation, (c) radiation. (d) Indicate the main limiting factor on temporal variation of St on the Tibetan Plateau. The bottom left insets in (a)–(c) show the frequency distributions of corresponding correlation coefficients, and the texts show the proportions of areas with positive (P) and negative (N) correlations, respectively. The texts in the lower left corner in (d) describe the proportions of the regions controlled by temperature (T2m), precipitation (Pre) and radiation (Rad), respectively.

nonexclusive, hence, further studies are needed to reveal the physiological process of vegetation dynamics to the variation of climatic factors. Moreover, the relationship between other phenological metrics (e.g., the end of growing season, EOS) and St needs to explore further. Therefore, we recommend further investigations on the impact of climatic change on St and vegetation phenology for various vegetation types at larger regions. This will help us better understand the mechanisms of responses and feedbacks of vegetation dynamics to climate change and our ability to accurately explain them through improved models.

V. Conclusion

This article assessed the spatio-temporal variation of spring phenology and temperature St response to preseason climate factors on the TP based on CSIF and meteorological reanalysis data. Our study confirmed the spatial pattern of distinct trends of SOS during 2001–2020, i.e., advanced (58.1%) and delayed (41.9%) trends were mainly distributed in the eastern and western TP, respectively. Moreover, this article also highlighted St has experienced a significant decrease with an average speed of 0.14 day/°C per year on the TP during 2001–2020. Spatially, St was positive in eastern TP but negative in western TP. The spatial distribution of St was much more affected by precipitation and air temperature, with a 1 mm decrease of precipitation and 1 °C warming incurring a decrease in St of 0.02 and 0.54 day/°C, respectively. Temporally, preseason climate factors synergistically contributed to the decrease of St. These findings have significant implications for understanding the response of spring phenology to climate change on the TP, and further confirms that preseason climate factors should be taken into account in spring phenology research models.

Appendix

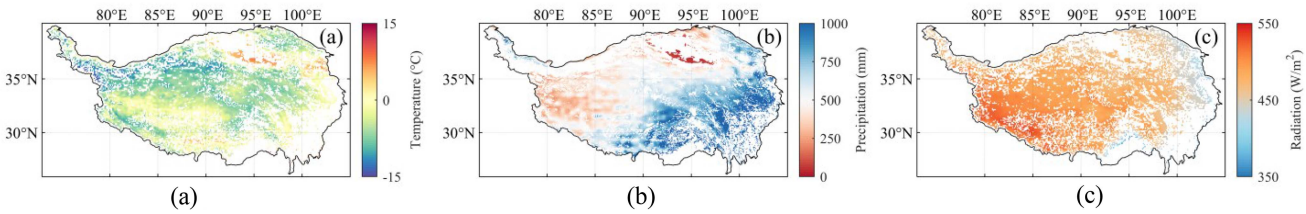

Fig. 8. Spatial pattern of multi-year averaged climate factors the Tibetan Plateau during 2001–2020. (a) Annual 365-days average temperature. (b) Annual 365-days accumulated average precipitation. (c) Annual 365-days average radiation.

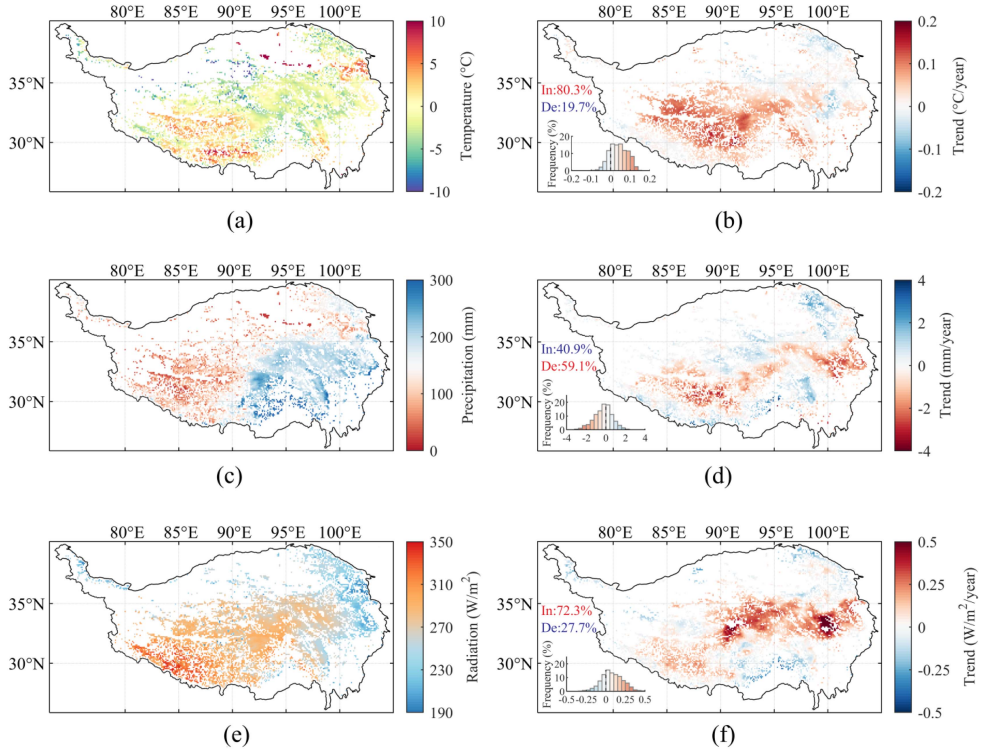

Fig. 9. Spatial pattern of preseason climate factors during 2001–2020 (a) Annual 365 days average temperature. (b) Trend of temperature. (c) Annual 365 days avera ge accumulated precipitation (d) Trend of precipitation. (e) Annual 365 days average radiation (f) Trend of radiation. The bottom left insets in (b), (d) and (f) show the corresponding frequency distributions. The texts show the proportions of areas with increased (In) and decreased (De) trend, respectively.

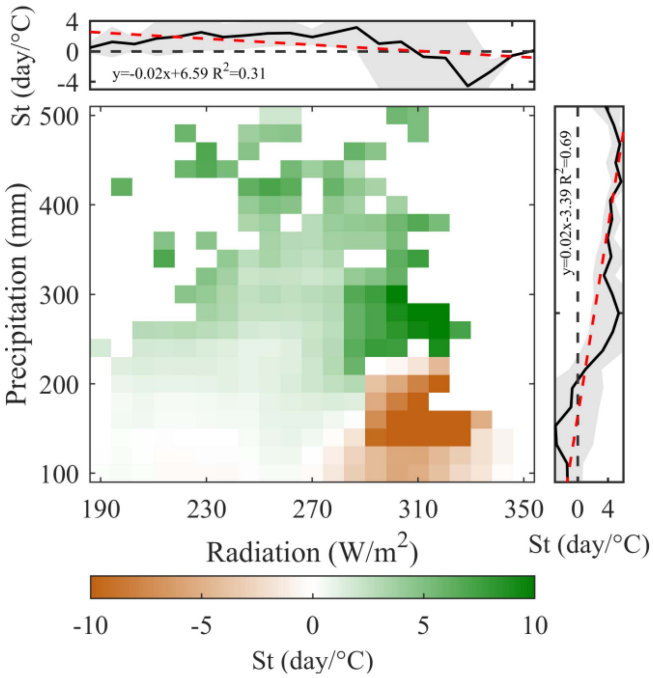

Fig. 10. Distribution of temperature sensitivity (St) in the climatic space composed of the preseason radiation and preseason precipitation during 2001–2020. In the upper and right subgraphs, the solid black lines indicate the St variations with radiation and precipitation, respectively. The gray shadows areas the standard deviation error of St in each bin, the dashed red lines are the fitted linear regressions, and the dashed black lines indicated the location of 0 day/°C.

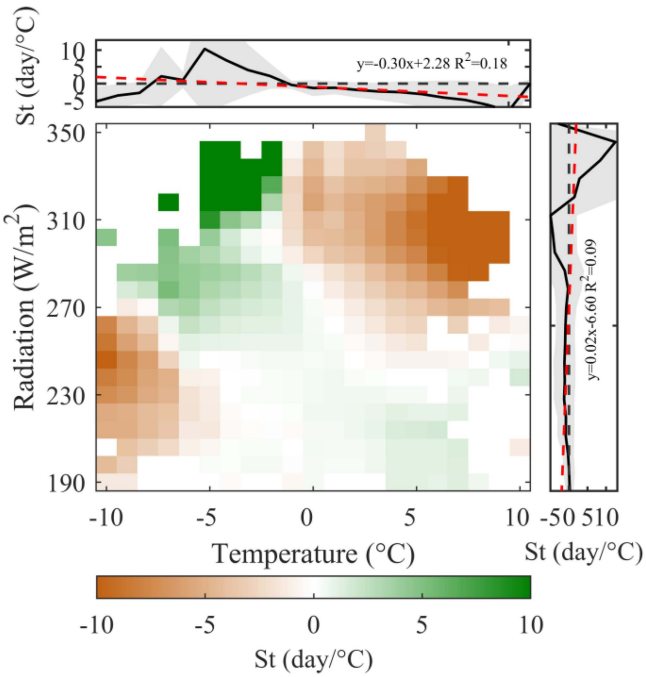

Fig. 11. Distribution of temperature sensitivity (St) in the climatic space composed of the preseason temperature and preseason radiation during 2001–2020. In the upper and right subgraphs, the solid black lines indicate the St variations with temperature and radiation, respectively. The gray shadows areas the standard deviation error of St in each bin, the dashed red lines are the fitted linear regressions, and the dashed black lines indicated the location of 0 day/°C.

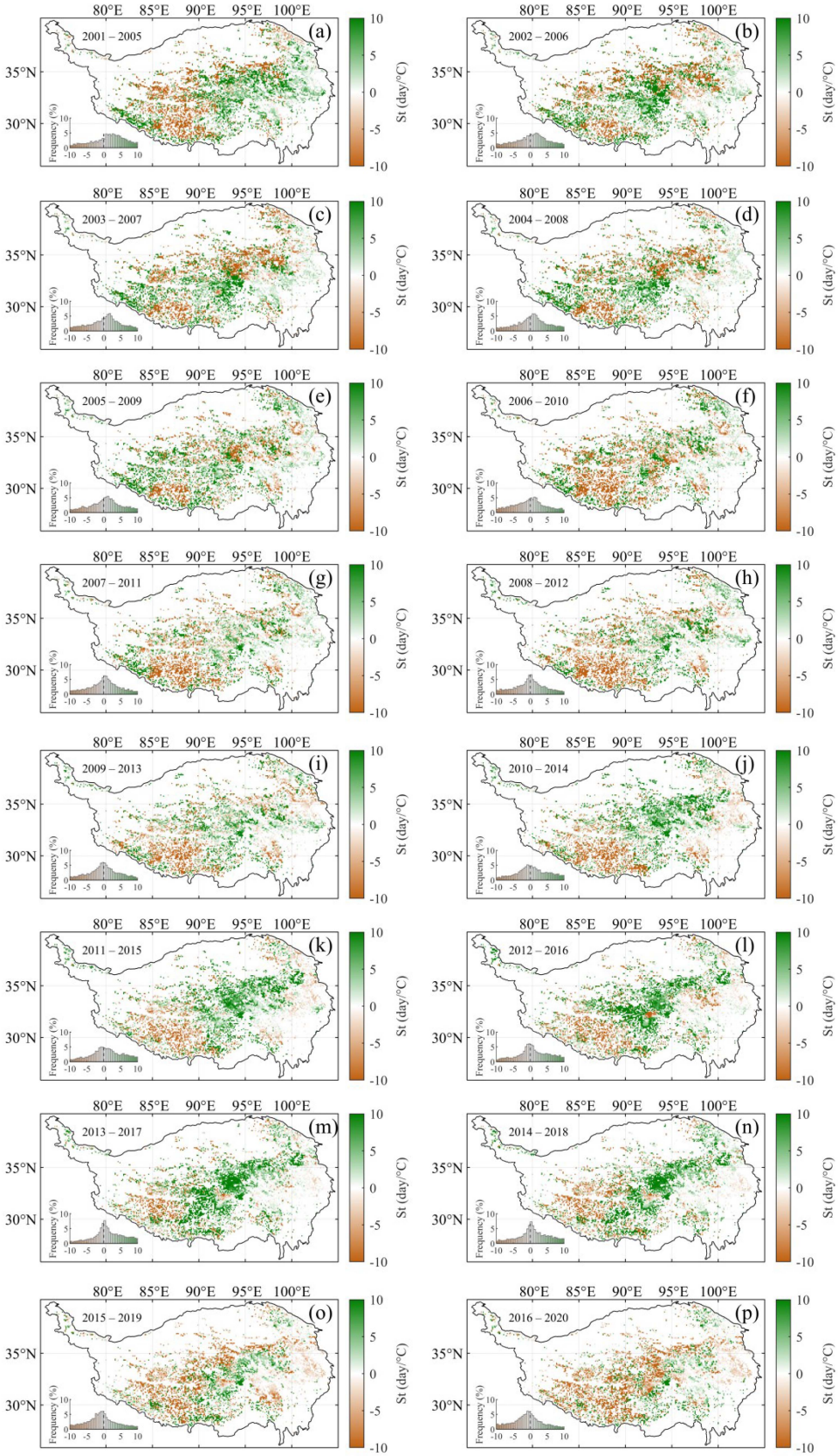

Fig. 12. Spatial pattern of temperature sensitivity (St) calculated by 5-year moving window. (a)–(p) St calculated for each window, which was represented on the top of subplot. The bottom left insets show the frequency distributions of corresponding St.

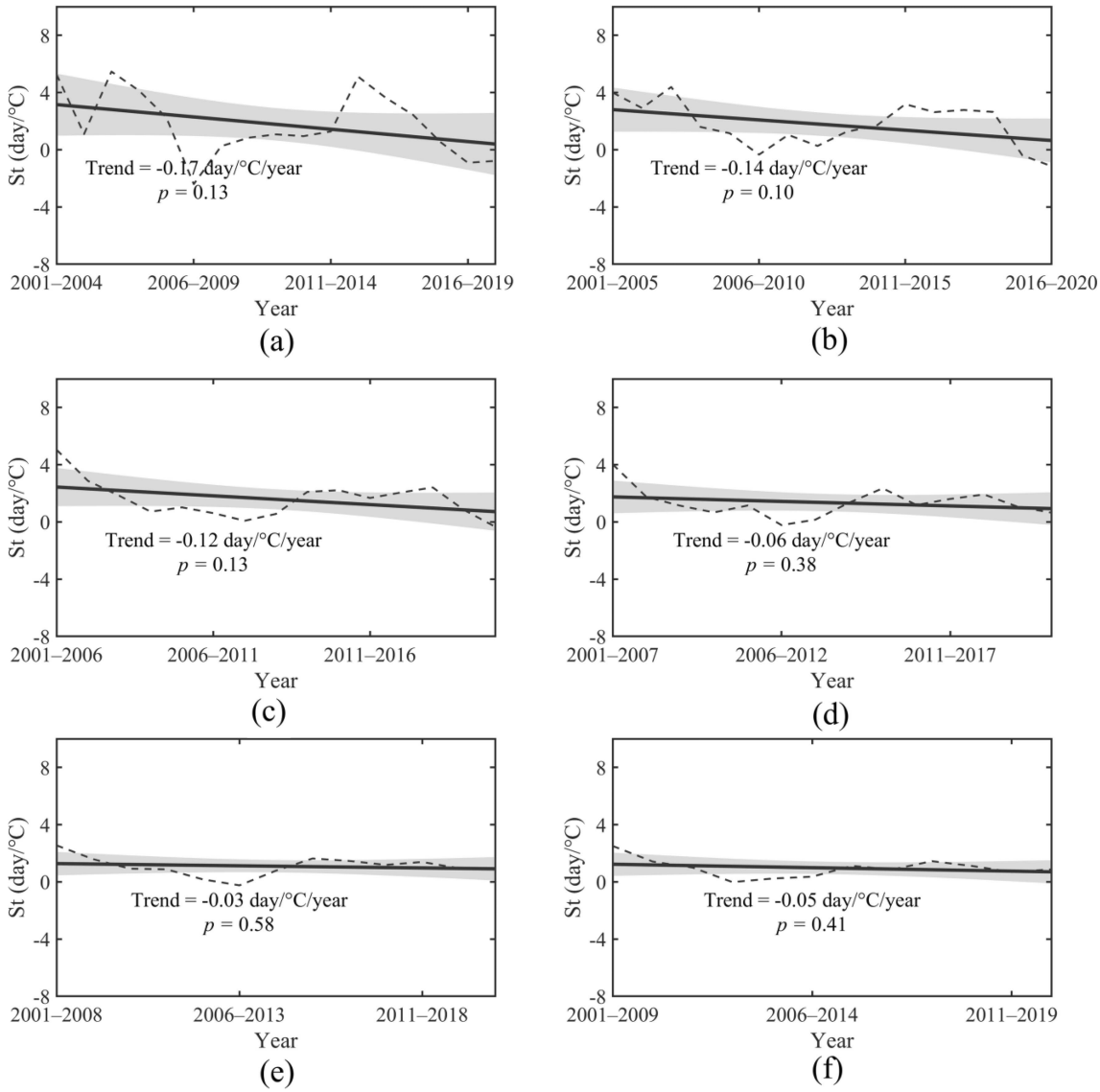

Fig. 13. Temporal variation of temperature sensitivity (St) with a (a) 4-year, (b) 5-year, (c) 6-year, (d) 7-year, (e) 8-year and (f) 9-year moving window on the Tibetan Plateau during 2001–2020.

ACKNOWLEDGMENT

The authors would like to thank the anonymous reviewers and the editor for their constructive comments and suggestions.

REFERENCES

[1] Y. H. Fu et al., "Declining global warming effects on the phenology of spring leaf unfolding," *Nature*, vol. 526, no. 7571, pp. 104–107, Oct. 2015.

[2] M. G. Shen, G. X. Zhang, N. Cong, S. P. Wang, W. D. Kong, and S. L. Piao, "Increasing altitudinal gradient of spring vegetation phenology during the last decade on the Qinghai-Tibetan Plateau," *Agricultural Forest Meteorol.*, vol. 189, pp. 71–80, Jun. 2014.

[3] G. R. Deng et al., "Asymmetric effects of daytime and nighttime warming on boreal forest spring phenology," *Remote Sens.,* vol. 11, no. 14, Jul. 2019, Art. no. 1651.

[4] M. Shen et al., "Plant phenology changes and drivers on the Qinghai–Tibetan Plateau," *Nature Rev. Earth Environ.*, vol. 3, pp. 633–651, Jul. 2022.

[5] J. Peng, C. Y. Wu, X. Y. Wang, and L. L. Lu, "Spring phenology outweighed climate change in determining autumn phenology on the Tibetan Plateau," *Int. J. Climatol.,* vol. 41, no. 6, pp. 3725–3742, May 2021.

[6] M. Y. Dong, Y. Jiang, C. T. Zheng, and D. Y. Zhang, "Trends in the thermal growing season throughout the Tibetan Plateau during 1960-2009," *Agricultural Forest Meteorol.,* vol. 166, pp. 201–206, Dec. 2012.

[7] S. L. Piao et al., "Altitude and temperature dependence of change in the spring vegetation green-up date from 1982 to 2006 in the Qinghai-Xizang Plateau," *Agricultural Forest Meteorol.,* vol. 151, no. 12, pp. 1599–1608, Dec. 2011.

[8] Z. T. Zheng, W. Q. Zhu, G. S. Chen, N. Jiang, D. Q. Fan, and D. H. Zhang, "Continuous but diverse advancement of spring-summer phenology in response to climate warming across the Qinghai-Tibetan Plateau," *Agricultural Forest Meteorol.,* vol. 223, pp. 194–202, Jun. 2016.

[9] G. Zhang, Y. Zhang, J. Dong, and X. Xiao, "Green-up dates in the Tibetan Plateau have continuously advanced from 1982 to 2011," *Proc. Nat. Acad. Sci. USA*, vol. 110, no. 11, pp. 4309–4314, Mar. 2013.

[10] C. Wang, R. Y. Cao, J. Chen, Y. H. Rao, and Y. H. Tang, "Temperature sensitivity of spring vegetation phenology correlates to within-spring warming speed over the Northern Hemisphere," *Ecol. Indicators,* vol. 50, pp. 62–68, Mar. 2015.

[11] M. Gao et al., "Three-dimensional change in temperature sensitivity of northern vegetation phenology," *Glob. Change Biol.*, vol. 26, no. 9, pp. 5189–5201, Sep. 2020.
[12] J. Du, Z. B. He, K. B. Piatek, L. F. Chen, P. F. Lin, and X. Zhu, "Interacting effects of temperature and precipitation on climatic sensitivity of spring vegetation green-up in arid mountains of China," *Agricultural Forest Meteorol.,* vol. 269, pp. 71–77, May 2019.
[13] F. D. Meng, L. Huang, A. P. Chen, Y. Zhang, and S. L. Piao, "Spring and autumn phenology across the Tibetan Plateau inferred from normalized difference vegetation index and solar-induced chlorophyll fluorescence," *Big Earth Data*, vol. 5, no. 2, pp. 182–200, May 2021.
[14] A. Chen, F. Meng, J. Mao, D. Ricciuto, and A. K. Knapp, "Photosynthesis phenology, as defined by solar-induced chlorophyll fluorescence, is overestimated by vegetation indices in the extratropical Northern Hemisphere," *Agricultural Forest Meteorol.*, vol. 323, 2022, Art. no. 109027.
[15] Y. Yang et al., "Divergent performances of vegetation indices in extracting photosynthetic phenology for Northern deciduous broadleaf forests," *IEEE Geosci. Remote Sens. Lett.,* vol. 19, 2022, Art. no. 2505405, doi: 10.1109/lgrs.2022.3182405.
[16] X. Li et al., "Solar-induced chlorophyll fluorescence is strongly correlated with terrestrial photosynthesis for a wide variety of biomes: First global analysis based on OCO-2 and flux tower observations," *Glob. Change Biol.,* vol. 24, no. 9, pp. 3990–4008, Sep. 2018.
[17] Y. Zhang, R. Commane, S. Zhou, A. P. Williams, and P. Gentine, "Light limitation regulates the response of autumn terrestrial carbon uptake to warming," *Nature Climate Change,* vol. 10, no. 8, Aug. 2020, Art. no. 739.
[18] D. L. Hao et al., "Adjusting solar-induced fluorescence to nadir-viewing provides a better proxy for GPP," *ISPRS J. Photogramm. Remote Sens.,* vol. 186, pp. 157–169, Apr. 2022.
[19] J. R. Zhang et al., "NIRv and SIF better estimate phenology than NDVI and EVI: Effects of spring and autumn phenology on ecosystem production of planted forests," *Agricultural Forest Meteorol.*, vol. 315, Mar. 2022, Art. no. 108819.
[20] M. G. Shen et al., "Greater temperature sensitivity of vegetation greenup onset date in areas with weaker temperature seasonality across the Northern Hemisphere," *Agricultural Forest Meteorol.,* vol. 313, Feb. 2022, Art. no. 108759.
[21] G. F. Yin, A. Verger, A. Descals, I. Filella, and J. Penuelas, "Nonlinear thermal responses outweigh water limitation in the attenuated effect of climatic warming on photosynthesis in Northern ecosystems," *Geophys. Res. Lett.,* vol. 49, no. 16, Aug. 2022, Art. no. e2022GL100096.
[22] K. W. Li et al., "Spring phenological sensitivity to climate change in the Northern Hemisphere: Comprehensive evaluation and driving force analysis," *Remote Sens.,* vol. 13, no. 10, May 2021, Art. no. 1972.
[23] T. Wang et al., "The influence of local spring temperature variance on temperature sensitivity of spring phenology," *Glob. Change Biol.*, vol. 20, no. 5, pp. 1473–1480, May 2014.
[24] S. Gusewell, R. Furrer, R. Gehrig, and B. Pietragalla, "Changes in temperature sensitivity of spring phenology with recent climate warming in Switzerland are related to shifts of the preseason," *Glob. Change Biol.*, vol. 23, no. 12, pp. 5189–5202, Dec. 2017.
[25] H. Chen, Q. Zhu, N. Wu, Y. Wang, and C. H. Peng, "Delayed spring phenology on the Tibetan Plateau may also be attributable to other factors than winter and spring warming," *Proc. Nat. Acad. Sci. USA*, vol. 108, no. 19, May 2011, Art. no. E93.
[26] M. Cheng, J. Jin, J. Zhang, H. Jiang, and R. Wang, "Effect of climate change on vegetation phenology of different land-cover types on the Tibetan Plateau," *Int. J. Remote Sens.,* vol. 39, no. 2, pp. 470–487, 2017.
[27] Z. N. Jin et al., "Temporal variability in the thermal requirements for vegetation phenology on the Tibetan Plateau and its implications for carbon dynamics," *Climatic Change,* vol. 138, no. 3-4, pp. 617–632, Oct. 2016.
[28] P. L. Li, Z. M. Hu, and Y. W. Liu, "Shift in the trend of browning in Southwestern Tibetan Plateau in the past two decades," *Agricultural Forest Meteorol.,* vol. 287, Jun. 2020, Art. no. 107950.
[29] A. Chen, L. Huang, Q. Liu, and S. Piao, "Optimal temperature of vegetation productivity and its linkage with climate and elevation on the Tibetan Plateau," *Glob. Change Biol.*, vol. 27, no. 9, pp. 1942–1951, May 2021.
[30] L. Zhang, T. Li, and J. Wu, "Deriving gapless CO2 concentrations using a geographically weighted neural network: China, 2014–2020," *Int. J. Appl. Earth Observ. Geoinf.*, vol. 114, 2022, Art. no. 103063.
[31] J. L. Li et al., "Satellite observed indicators of the maximum plant growth potential and their responses to drought over Tibetan Plateau (1982-2015)," *Ecol. Indicators,* vol. 108, Jan. 2020, Art. no. 105732.
[32] X. Wang, C. Wu, D. Peng, A. Gonsamo, and Z. Liu, "Snow cover phenology affects alpine vegetation growth dynamics on the Tibetan Plateau: Satellite observed evidence, impacts of different biomes, and climate drivers," *Agricultural Forest Meteorol.,* vol. 256-257, pp. 61–74, 2018.
[33] Y. Zhang, J. Joiner, S. H. Alemohammad, S. Zhou, and P. Gentine, "A global spatially contiguous solar-induced fluorescence (CSIF) dataset using neural networks," *Biogeosciences,* vol. 15, no. 19, pp. 5779–5800, Oct. 2018.
[34] J. Muñoz-Sabater et al., "ERA5-land: A state-of-the-art global reanalysis dataset for land applications," *Earth Syst. Sci. Data,* vol. 13, no. 9, pp. 4349–4383, 2021.
[35] Y. Chen et al., "Spatial performance of multiple reanalysis precipitation datasets on the southern slope of central Himalaya," *Atmos. Res.,* vol. 250, 2021, Art. no. 105365.
[36] Q. Liu et al., "Delayed autumn phenology in the Northern Hemisphere is related to change in both climate and spring phenology," *Glob. Change Biol.*, vol. 22, no. 11, pp. 3702–3711, Nov. 2016.
[37] L. L. Zeng, B. D. Wardlow, D. X. Xiang, S. Hu, and D. R. Li, "A review of vegetation phenological metrics extraction using time-series, multispectral satellite data," *Remote Sens. Environ.,* vol. 237, Feb. 2020, Art. no. 111511.
[38] J. Zhou, L. Jia, and M. Menenti, "Reconstruction of global MODIS NDVI time series: Performance of harmonic analysis of time series (HANTS)," *Remote Sens. Environ.,* vol. 163, pp. 217–228, Jun. 2015.
[39] Q. Zhang, D. D. Kong, P. J. Shi, V. P. Singh, and P. Sun, "Vegetation phenology on the Qinghai-Tibetan Plateau and its response to climate change (1982-2013)," *Agricultural Forest Meteorol.,* vol. 248, pp. 408–417, Jan. 2018.
[40] H. Yu, E. Luedeling, and J. Xu, "Winter and spring warming result in delayed spring phenology on the Tibetan Plateau," *Proc. Nat. Acad. Sci. USA*, vol. 107, no. 51, pp. 22151–22156, Dec. 2010.
[41] Q. Xie et al., "Land surface phenology retrievals for arid and semi-arid ecosystems," *ISPRS J. Photogramm. Remote Sens.,* vol. 185, pp. 129–145, 2022.
[42] P. S. A. Beck, C. Atzberger, K. A. Hogda, B. Johansen, and A. K. Skidmore, "Improved monitoring of vegetation dynamics at very high latitudes: A new method using MODIS NDVI," *Remote Sens. Environ.,* vol. 100, no. 3, pp. 321–334, Feb. 2006.
[43] A. Gonsamo, J. M. Chen, and P. D'Odorico, "Deriving land surface phenology indicators from CO2 eddy covariance measurements," *Ecol. Indicators,* vol. 29, pp. 203–207, Jun. 2013.
[44] X. Zhang et al., "Monitoring vegetation phenology using MODIS," *Remote Sens. Environ.,* vol. 84, no. 3, pp. 471–475, 2003.
[45] G. F. Yin, A. Verger, I. Filella, A. Descals, and J. Penuelas, "Divergent estimates of forest photosynthetic phenology using structural and physiological vegetation indices," *Geophys. Res. Lett.*, vol. 47, no. 18, Sep. 2020, Art. no. e2020GL089167.
[46] T. F. Keenan, A. D. Richardson, and K. Hufkens, "On quantifying the apparent temperature sensitivity of plant phenology," *New Phytologist*, vol. 225, no. 2, pp. 1033–1040, Jan. 2020.
[47] J. Wang et al., "Contrasting temporal variations in responses of leaf unfolding to daytime and nighttime warming," *Glob. Change Biol.,* vol. 27, no. 20, pp. 5084–5093, Oct. 2021.
[48] W. G. Jiang, L. H. Yuan, W. J. Wang, R. Cao, Y. F. Zhang, and W. M. Shen, "Spatio-temporal analysis of vegetation variation in the Yellow River Basin," *Ecol. Indicators,* vol. 51, pp. 117–126, Apr. 2015.
[49] Z. Z. Liu, H. Wang, N. Li, J. Zhu, Z. W. Pan, and F. Qin, "Spatial and temporal characteristics and driving forces of vegetation changes in the Huaihe River Basin from 2003 to 2018," *Sustainability*, vol. 12, no. 6, Mar. 2020, Art. no. 2198.
[50] Q. F. Gronau, A. Ly, and E.-J. Wagenmakers, "Informed Bayesian t-tests," *Amer. Statistician,* vol. 74, no. 2, pp. 137–143, 2019, doi: 10.1080/00031305.2018.1562983.
[51] M. Shen, S. Piao, N. Cong, G. Zhang, and I. A. Jassens, "Precipitation impacts on vegetation spring phenology on the Tibetan Plateau," *Glob. Change Biol.*, vol. 21, no. 10, pp. 3647–3656, Oct. 2015.
[52] J. Sun, X. Qin, and J. Yang, "The response of vegetation dynamics of the different alpine grassland types to temperature and precipitation on the Tibetan Plateau," *Environ. Monit. Assessment,* vol. 188, no. 1, Jan. 2016, Art. no. 20.
[53] M. G. Shen et al., "Plant phenological responses to climate change on the Tibetan Plateau: Research status and challenges," *Nat. Sci. Rev.,* vol. 2, no. 4, pp. 454–467, Dec. 2015.

[54] J. A. Klein, K. A. Hopping, E. T. Yeh, Y. Nyima, R. B. Boone, and K. A. Galvin, "Unexpected climate impacts on the Tibetan Plateau: Local and scientific knowledge in findings of delayed summer," *Glob. Environ. Change-Hum. Policy Dimension,* vol. 28, pp. 141–152, Sep. 2014.
[55] F. F. Yu, K. P. Price, J. Ellis, and P. J. Shi, "Response of seasonal vegetation development to climatic variations in eastern central Asia," *Remote Sens. Environ.,* vol. 87, no. 1, pp. 42–54, Sep. 2003.
[56] Y. S. H. Fu, M. Campioli, G. Deckmyn, and I. A. Janssens, "Sensitivity of leaf unfolding to experimental warming in three temperate tree species," *Agricultural Forest Meteorol.,* vol. 181, pp. 125–132, Nov. 2013.
[57] S. Piao et al., "Plant phenology and global climate change: Current progresses and challenges," *Glob. Change Biol.*, vol. 25, no. 6, pp. 1922–1940, Jun. 2019.
[58] L. Chen et al., "Spring phenology at different altitudes is becoming more uniform under global warming in Europe," *Glob. Change Biol.*, vol. 24, no. 9, pp. 3969–3975, Sep. 2018.
[59] A. Kleidon and M. Renner, "A simple explanation for the sensitivity of the hydrologic cycle to surface temperature and solar radiation and its implications for global climate change," *Earth Syst. Dyn.,* vol. 4, no. 2, pp. 455–465, 2013.
[60] N. Cong, Y.-J. Zhang, and J.-T. Zhu, "Temperature sensitivity of vegetation phenology in spring in mid- to high-latitude regions of Northern Hemisphere during the recent three decades," *Chin. J. Plant Ecol.,* vol. 46, no. 2, pp. 125–135, 2022.
[61] X. Wang et al., "Has the advancing onset of spring vegetation green-up slowed down or changed abruptly over the last three decades?," *Glob. Ecol. Biogeography,* vol. 24, no. 6, pp. 621–631, 2015.

Zhangkai Chen received the B.S. degree in remote sensing science and technology from Chengdu University of Information Technology, Chengdu, China, in 2021. He is currently working toward the M.S. degree in surveying and mapping with the Faculty of Geosciences and Environmental Engineering, Southwest Jiaotong University, Chengdu, China.

His research interests include remote sensing of vegetation phenology and alpine treeline dynamics.

Rui Chen received the B.S. degree in surveying and mapping engineering from the China University of Petroleum (East China), Qingdao, China, in 2019. He is currently working toward the Ph.D. degree in surveying and mapping with the Faculty of Geosciences and Environmental Engineering, Southwest Jiaotong University, Chengdu, China.

His research interests include topographic correction for optical optical remote sensing images.

Yajie Yang received the B.S. degree in remote sensing science and technology in 2020 from Southewest Jiaotong University, Chengdu, China, where she is currently working toward the M.S. degree in surveying and mapping with the Faculty of Geosciences and Environmental Engineering.

Her research interests include remote sensing of vegetation phenology.

Huiqin Pan received the B.S. degree in surveying and mapping engineering from Henan Polytechnic University, Henan, China, in 2020. She is currently working toward the M.S. degree in surveying and mapping with the Faculty of Geosciences and Environmental Engineering, Southwest Jiaotong University, Chengdu, China.

Her research interests include remote sensing of vegetation phenology.

Qiaoyun Xie received the Ph.D. degree in cartography and geographic information system from the Chinese Academy of Sciences, Beijing, China, and University of Southampton, Southampton, United Kingdom, in 2017.

She is specializes in vegetation monitoring and their interactions with climate. She is a Lecturer with the School of Engineering, University of Western Australia, Crawley, WA, Australia. Her research interests include using satellite and ground data for vegetation dynamics monitoring, vegetation parameter retrieval, vegetation phenology and their shifting seasonality with climate variability.

Cong Wang received the B.S. degree in remote sensing science and technology from Wuhan University, Wuhan, China, in 2014 and the Ph.D. degree in cartography and geographic information system from Aerospace Information Research Institute, Chinese Academy of Sciences, Beijing, China, in 2020.

She is currently a Lecturer with the College of Urban and Environmental Sciences, Central China Normal University, Wuhan, China. Her research interests include land surface dynamics, climate-terrestrial ecosystem interaction.

Baodong Xu received the Ph.D. degree in cartography and geographic information system from the Institute of Remote Sensing and Digital Earth, Chinese Academy of Sciences, in 2018.

Since 2018, he has been an Associate Professor with the Macro Agriculture Research Institute, College of Resources and Environment, Huazhong Agricultural University, Wuhan, China. His research interests include biophysical variables estimation, validation of remote sensing products, and remote sensing applications in agriculture.

Gaofei Yin (Senior Member, IEEE) received the Ph.D. degree in cartography and geographic information system from the Institute of Remote Sensing and Digital Earth, Chinese Academy of Sciences, Beijing, China, in 2015.

From 2019 to 2021, he was a Marie Skłodowska-Curie Individual Fellow with the Global Ecology Unit, Center for Ecological Research and Forestry Applications, Barcelona, Spain. He is currently a Professor with the Faculty of Geosciences and Environmental Engineering, Southwest Jiaotong University, Chengdu, China. His current research interests include vegetation remote sensing, and global change ecology.

Dr. Yin is currently an Associated Editor for IEEE GEOSCIENCE AND REMOTE SENSING LETTERS.